КОМП'ЮТЕРНІ НАУКИ

UDC 519.87:550.34+53.082.4:[69.058:271.2-788(477.411)]
DOI: https://doi.org/10.17721/ISTS.2024.8.74-84

Vasyl MOSTOVYY, DSc (Phys. & Math.), Leading Researcher
ORSID ID: 0000-0002-1759-1893
e-mail: vasyl.mostovyy@gmail.com
Taras Shevchenko National University of Kyiv, Kyiv, Ukraine

MATHEMATICAL MODEL OF THE SIGNAL EMISSION DYNAMICS IN SEISMIC-ACOUSTIC MONITORING SYSTEMS OF BUILDING STRUCTURES

Background. *The paper presents a mathematical model of automated systems of seismoacoustic monitoring of building structures to assess the dynamics of crack formation in building structures to prevent the destruction of the objects under investigation. The seismoacoustic field generated by the research objects is reflected in the matrix of informative parameters, the dynamics of which characterize the dynamics of the object's state. To assess the dynamics of high-frequency signals generated by cracks that occur during the operation of the structure, it is advisable to use the dynamics of emissions that generate these signals. For this, from the point of view of physical practicality, it makes sense to choose a model that characterizes the dynamics of the high-frequency range of the spectrum. Namely, the work presents an algorithm based on a theorem for stationary processes in a broad sense.*

Methods. *The aging process can be reflected in the feature space, which can be reduced to parameters characterizing the elastic properties of the materials that form the objects under study. Since the propagation velocities and the shape of longitudinal and transverse waves in the material depend on the elastic parameters of these materials (Poisson's ratio and Young's modulus), the change in these parameters leads to changes in the spectral characteristics of the emission signals that occur in the aging material. Any redistribution of energy in the material is accompanied by the appearance of signals that generate emission. The dynamics of the parameters of the emission signal reflect the change in the elastic properties of the object under study. Possible reasons for changes in the internal structure are the appearance and growth of cracks, phase transitions in monolithic materials, and loosening of components. This means that changes in the dynamic parameters of emission signals are related to the dynamic characteristics of this object.*

Results. *A mathematical model of building structure aging is proposed. This model of aging of the object must consider the nature of external influences on the object and the nature of its reaction to external disturbances. Given stochastic background noise during monitoring, only the statistical nature of this dependence should be accepted in the model. This model is implemented in building № 3 (cell) of the Kyiv Pechersk Lavra.*

Conclusions. *Two stages of the study of the emission dynamics of building № 3 of the Kyiv Pechersk Lavra showed that during the given time interval, the change in the emission characteristics of this object is within the measurement error. Thus, for an adequate assessment of the emission dynamics generated by cracks that arise during the KPL hull No. 3 operation, it is necessary to collect statistics over a time interval of several decades. To solve this problem, it is essential to carry out permanent seismoacoustic monitoring of the building structure.*

Keywords: *seismoacoustic monitoring, seismoacoustic emission, mathematical model, seismoacoustic signal, matrix of informative parameters of the model, aging of structures.*

Background

The dynamics of emission signal parameters reflect changes in the elastic properties of the object under investigation. This means that changes in the dynamic parameters of emission signals are related to the dynamic characteristics of this object. Given the presence of stochastic background noise during monitoring, only the statistical nature of this dependence should be accepted in the model. The key issue is the selection of informative parameters for the space of signs, in which it is necessary to carry out a dynamic analysis of their behavior, on the basis of which to build a decisive rule for forecasting the state of the object (Mostovyy, V., 2013). There is a problem of choosing the space of signs of aging and fatigue. Since we have only indirect information about the state of the object in the form of the characteristics of the emitted signals, we will be able to make only indirect measurements related to the propagation of emission waves. Dynamic changes of these waves are reflected in the dynamics of their spectral characteristics. The space of spectral characteristics is based on parameters statistically related to the characteristics of the object. The stochastic characteristics of such a component random process reflect the process of changing the elastic characteristics of the material. The task of estimating the parameters of the analyzed random process is reduced to estimating their posterior probability, the dynamics of which reflect fatigue and the aging process of the object.

Passive seismic-acoustic monitoring of construction objects is understood as routine observation of parameters of the natural background of the investigated object. The natural background of the object is a superposition of emission signals caused by natural changes of the object under study (the appearance of microcracks, etc.) and the object's response to external disturbance (wind loads, the impact of transport, seismic events, soil vibrations caused by the vibrations of objects of various nature, the reaction of these objects to external actions, etc.). The mathematical model of object aging should consider the nature of external influences on the object and the nature of its reaction to external disturbances.

Passive seismic-acoustic monitoring will be used to observe the dynamics of the parameters of the mathematical model of the research process and assess the state of aging of the object under study.

Methods

The aging process, a crucial aspect in the life cycle of building structures, is reflected in the feature space. This space can be reduced to a set of parameters characterizing the elastic properties of the materials. Understanding how changes in these parameters lead to changes in the spectral characteristics of the emission signals is key to predicting and managing structural health.

ISSN 2707-1758

The natural frequencies of the investigated objects were in the seismic frequency range. In the stationary state of the object, steady migration of the vector characterizing the state of the object was observed in the space of features within the ellipsoid of rotation of a relatively small volume as passive monitoring. This circumstance is related to the stochastic nature of the monitoring process. This state, crucially, is observed before the onset of fatigue. From the point of view of materials science, fatigue is local structural damage that develops and occurs during cyclic loads on the material. The maximum stress values in the cycle are less than the highest stress limit and below the stress limit for the given material.

The structural failure of the material, a critical event, consists in the loss of the load-bearing capacity of the element or directly of the entire structure. It begins when the stresses in the material approach the limit, causing excessive deformations, when the material in the process of a complete cycle returns to its initial state, i.e., the phenomenon of hysteresis is manifested. Any energy redistribution in the material, a key factor, is accompanied by the emergence of emitted signals. Emission signals, the focus of our study, are voltage waves generated by a sudden internal redistribution of voltage in the material caused by changes in the internal structure.

Possible reasons for changes in the internal structure: the appearance and growth of cracks, phase transitions in monolithic materials and loosening of components.

Structural analysis and identification of dynamic parameters of building structures and their components whose spectral characteristics lie in the seismic and lower part of the acoustic ranges are extremely important in their monitoring to predict significant changes in dynamic characteristics. By geometric dimensions, they are large artificial and natural objects. The method of dynamic identification provides an opportunity to investigate the dynamic behavior of this structure with the help of non-destructive tests and, therefore, allows us to assess the "health" of the structure and the possible need for more detailed monitoring. The method of examination of the response of the structure to the dynamic load is analyzed, which can be any environmental (wind, sea waves, traffic, etc.) or artificially caused using test pulses.

Of particular interest is the passive monitoring of objects with sources of emission signals, the parameters of which are subject to determination and characteristic of the structure. The emission can be both irregular and regular. In the latter case, it can be modeled as a flow with probabilistic characteristics to be determined (Mostovyy, V., 2013).

A change in the condition of building structures during their operation can lead to undesirable and sometimes even catastrophic consequences. The cause of destruction of engineering structures and their components is most often structural changes of composite materials, under which destruction occurs in operational loads and natural aging (Schijve, 2003). An example of such consequences can be the well-known, relatively recent collapses of building structures in Germany, Japan, France, Latvia, and the USA (such as the collapse of the city archive building in Cologne on March 3, 2009, the collapse of a car tunnel near Tokyo on December 2, 2012, the collapse of the terminal at Charles de Gaulle Airport on 05/24/2004, the collapse of the Maxim center in Riga on 11/21/2013, the collapse of a residential building in Miami, Florida, USA on 06/24/2021) and many other countries. In Ukraine, an example of such a disaster can be the collapse of a building on the street. Hrushevsky in the city of Drohobych, 28.08.2019, the bridge's destruction in Kharkiv on 30.08. 2019, and others. Continuous seismic-acoustic monitoring makes it possible to evaluate the dynamics of the strength characteristics (Young's modulus and shear modulus) of the object under investigation to forecast its condition (Tassios, 2010).

To study the dynamics of parameters characterizing the strength parameters of building structures, a new concept of seismic-acoustic monitoring of natural and building objects is proposed, in which the object under investigation is mapped into an n-dimensional vector of the Euclidean space of informative parameters using a physically feasible parametric model. For seismic-acoustic monitoring of building structures, a mathematical model (Mostovyy, V., 2013) was used within the framework of this concept in order to assess the dynamics of the object's parameters characterizing its strength (Mostovyy, V., 2013).

The monitoring concept was based on the following physical principles. Since the speed of propagation and the form of longitudinal and transverse waves in the material depend on the elastic parameters of these materials, the change in these parameters leads to changes in the spectral characteristics of the emission signals that occur in the aging material. The emission refers to the redistribution of energy in the material, accompanied by the appearance of emitted signals. Signal emissions are stress waves generated by a sudden internal redistribution of stress in the material caused by changes in the internal structure, i.e., material fatigue. The emission is caused by the redistribution of energy in the material. Any energy redistribution in the material is accompanied by the emergence of emitted signals. The superposition of such signals generates an emission field (Tassios, 2010).

From the point of view of material science, fatigue is developing, and local structural damage occurs during cyclic loads on the material (Suresh, 2004). Cyclic stress should lead to material fatigue. Fatigue leads to irreversible deformations of the material, that is, to its aging. The aging process in the proposed models is a change in material parameters that are reflected in the feature space. Parameterization of the analyzed process takes place using its approximation of a parametric model with free parameters. Thus, the process of seismic-acoustic monitoring of natural and building structures is reduced to regular observations of the free parameters of the selected model.

The physical principles of seismic-acoustic monitoring presented above in an actual embodiment require the researcher to solve complex mathematical problems. From the registration of the implementation of the emission field to the estimation of the free parameters of the model, a complex mathematical apparatus is used, which is based on such mathematical disciplines as the theory of random processes, functional analysis, the theory of the function of a complex variable, linear algebra, optimization methods and the theory of decision making (Timoshenko, & Gere, 1961), which is presented in the study of the dynamics of the state of building structures.

Since the propagation velocity of longitudinal and transverse waves are functions of the characteristics of the medium's strength, namely Young's modulus and the shear modulus, respectively, it is physically appropriate to use the medium's spectral characteristics as informative parameters of the mathematical model of the object under study.

Thus, wave propagation dynamics characterize the dynamics of the strength characteristics, and a change in the state of the research object itself causes the departure from the stationarity of the spectral characteristics (Mostovoy, V., & Mostovoy, S., 2023).

Mathematical model of the signal emission dynamics. To assess the dynamics of high-frequency signals generated by cracks that arise during the operation of the structure, it is advisable to use the dynamics of emissions that generate these signals. For this, from the point of view of physical practicality, it makes sense to choose a model that characterizes the dynamics of the high-frequency range of the spectrum. Namely, the algorithm is based on a theorem for stationary in the sense of processes. If a stationary process in a broad sense has a completely entirely continuous spectrum and the spectral density of the process allows the representation

$$f(\omega) = (h(i\omega)^2 \quad (1)$$

here

$$h(i\omega) = \int_0^\infty b(\tau) \cdot \exp(-i \cdot \omega \cdot \tau) d\tau,$$

$$\int_0^\infty (b(\tau)(^2 \cdot d\tau \angle \infty. \quad (2)$$

then the process is the response of a physically feasible filter $a(t)$ and

$$h(i\omega) = \sqrt{\frac{1}{2 \cdot \pi}} \cdot \int_0^\infty a(\tau) \cdot \exp(i \cdot \omega \cdot \tau) \cdot d\tau. \quad (3)$$

The detection algorithm follows from this. On the prehistory T, under the assumption of stationarity in the broad sense of a stochastic process $n(t)$ we estimate its spectral density $h(i\omega)$ and map it into a vector of the n-dimensional parameter $\vec{h}$ space, for example, by calculating the energy of the spectral density $h(i\omega)$ in n subbands (ω_i, ω_{i+1}) $i = \overline{1,n}$, and then estimate in the Euclidean metric the deviation of the vector $\vec{h}_t$ calculated in the sliding window from $\vec{h}$:

$$\left\| \vec{h}_t - \vec{h} \right\| \le H. \quad (4)$$

If this expression is correct, a decision is made about the absence of negative dynamics of the research object. Otherwise, the fragment of the process $(t, t+T)$ characterizes the negative dynamics of the aging process. The setpoint level H is determined by the researcher, who determines the setpoint level in terms of its probability of false alarm and target miss.

Application of a mathematical model to assess the impact of emission processes on the dynamics of the state of building № 3 (cell) of the Kyiv Pechersk Lavra. Seismic-acoustic monitoring of the microseismic background of critical points of the objects under investigation is conducted to obtain the spectral characteristics of the building № 3 (cell) of the Kyiv Pechersk Lavra under investigation and to analyze the observed data to forecast the dynamics of the object under investigation. A specialized seismic recorder, ZIR-2, developed and produced by the Ukrainian company "Roden", was used to record vibrations. The spectral ranges of the sensors are 0.5–600 Hz. It should be noted that the spectrum of the object under study is its stable characteristic, which changes when the mechanical parameters of the structure change, and it can be used to detect "age-related" changes in the structure during its life. It can be assumed that the fixed spectral characteristics of the structure can further be used as the set starting values for detecting the moment of its "aging", which can change during the monitoring process in case of accumulation of local damages.

The work's purpose is to evaluate the dynamics of high-frequency signals generated by cracks that occur during the operation of a building № 3 (cell) of the Kyiv Pechersk Lavra structure.

To evaluate the dynamics of high-frequency signals generated by cracks that occur during the operation of the building structure under investigation. To evaluate the dynamics of high-frequency signals generated by cracks that occur during the operation of the building structure under investigation, let us compare two observations of registered data. A significant change in the model parameters for two dimensions indicates a strong cracking emission, which can lead to undesirable consequences for the operation of the building structure under study.

The first observation. To assess the dynamics of the emission intensity generated by cracking in the observation area, we will carry out the first observations using the parametric model (1–4), Fig. 1–4. The dynamics of the parameters of this model will characterize the dynamics of emission of crack formation in the structure of building # 3 (cell) of the Kyiv Pechersk Lavra under study.

The first observation of the building № 3 (cell) of the Kyiv Pechersk Lavra is given below.

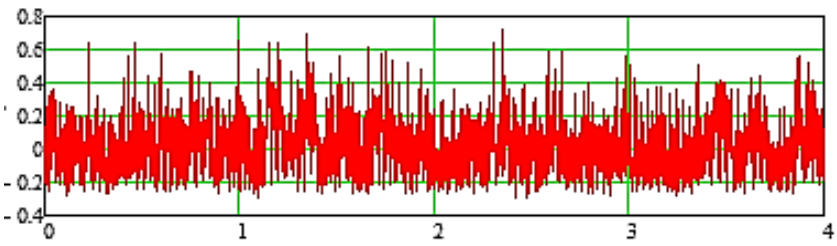

Fig. 1. A fragment of the recording of the first observation (duration 4 seconds) of the building's reaction to the natural background. The abscissa shows time in seconds. Along the ordinate axis, the function of the acceleration of the structure's oscillations in m/sec^2 is plotted with precision to the multiplier

Data registration during seismic-acoustic monitoring is accompanied by simultaneous additive interference caused by external factors. This study used frequency filtering for data preprocessing (Mostovoy, S., & Mostovoy, V., 2011).

Figures 1 and 2 show fragments of the recording of the first observation lasting 4 seconds, the response of the building № 3 (cell) of the Kyiv Pechersk Lavra to the natural background, unfiltered (Fig. 1) and filtered (Fig. 2).

ISSN 2707-1758

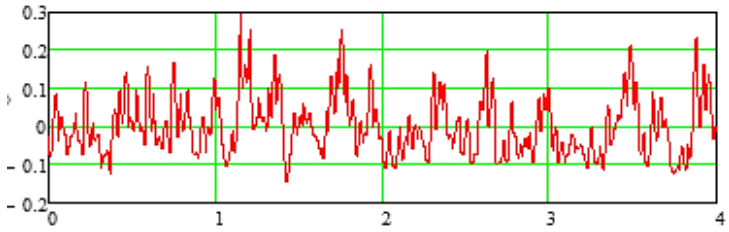

Fig. 2. A fragment of a filtered recording of the first observation (duration 4 seconds) of the building's reaction to the natural background. On the abscissa axis, the time is present in seconds. Along the ordinate axis, the function of the acceleration of oscillation of the structure m/sec^2 is plotted with precision to the multiplier

The Figure 3 shows the Amplitude of the module of the Fourier spectrum of the low-pass filtered data of building № 3 (cell) of the Kyiv Pechersk Lavra seismic records.

The frequency range was from 90 Hz to 500 Hz. It was divided into five equal quantiles (4), each into five equal subranges.

The Figure 4 shows the Fourier amplitude of the filtered data of the first range of the first observation of building № 3 (cell) of the Kyiv Pechersk Lavra. The energy of each of the twenty sub bands was presented in a matrix of the first observation 5×5.

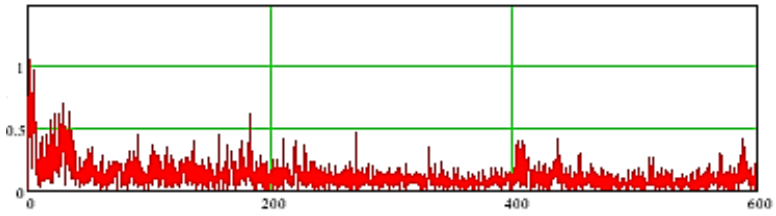

Fig. 3. The amplitude of the module of the Fourier spectrum of the filtered data of the first observation in relative units, in the frequency range from 0 to 600 Hz. The frequency in Hertz is given on the abscissa. The y-axis shows the range amplitude in relative units

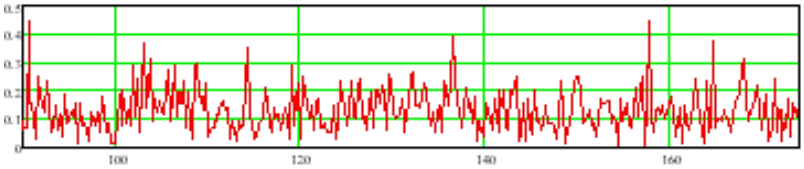

Fig. 4. The amplitude of the module of the Fourier spectrum of the filtered data of the first range in relative units, in the frequency range from 90 to 170 Hz. The frequency in Hertz is given on the abscissa. The y-axis shows the range amplitude in relative units

The Figure 5 shows the amplitude of the module of the Fourier spectrum of the filtered data of the first subband of the first band presented in relative units, in the frequency range from 90 to 105 Hz.

The Figure 6 shows the amplitude of the module of the Fourier spectrum of the filtered data of the second subband of the first band presented in relative units, in the frequency range from 105 to 125 Hz.

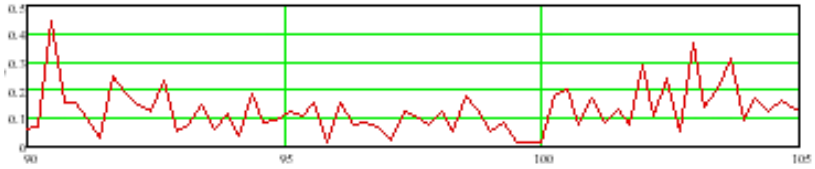

Fig. 5. The amplitude of the module of the Fourier spectrum of the filtered data of the first subband of the first band in relative units, in the frequency range from 90 to 105 Hz. The frequency in Hertz is given on the abscissa. The y-axis shows the range amplitude in relative units

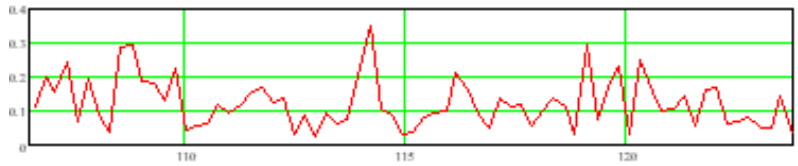

Fig. 6. The amplitude of the module of the Fourier spectrum of the filtered data of the second subband of the first band in relative units, in the frequency range from 105 to 125 Hz. The frequency in Hertz is given on the abscissa. The y-axis shows the range amplitude in relative units

The Figure 7 shows the amplitude of the module of the Fourier spectrum of the filtered data of the third subband of the first band presented in relative units, in the frequency range from 125 to 140 Hz.

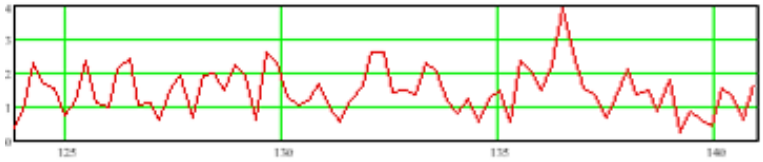

Fig. 7. The amplitude of the module of the Fourier spectrum of the filtered data of the third subband of the first band in relative units, in the frequency range from 125 to 140 Hz. The frequency in Hertz is given on the abscissa. The y-axis shows the range amplitude in relative units

The Figure 8 shows the amplitude of the module of the Fourier spectrum of the filtered data of the fourth subband of the first band presented in relative units, in the frequency range from 140 to 155 Hz.

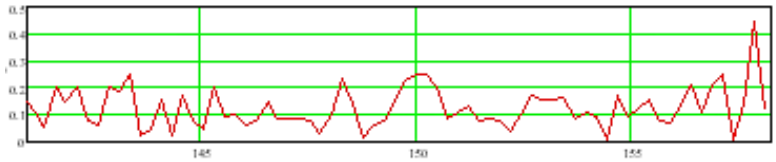

Fig. 8. The amplitude of the module of the Fourier spectrum of the filtered data of the fourth subband of the first band in relative units, in the frequency range from 140 to 155 Hz. The frequency in Hertz is given on the abscissa. The y-axis shows the range amplitude in relative units

The Figure 9 shows the amplitude of the module of the Fourier spectrum of the filtered data of the fourth subband of the first band presented in relative units, in the frequency range of 155 to 170 Hz.

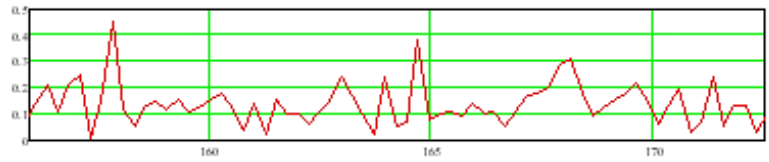

Fig. 9. The amplitude of the module of the Fourier spectrum of the filtered data of the fourth subband of the first band in relative units, in the frequency range from 155 to 170 Hz. The frequency in Hertz is given on the abscissa. The y-axis shows the range amplitude in relative units

The Figure 10 shows the Fourier amplitude of the filtered data of the first range of the first observation. The energy of each of the twenty subbands was presented in a matrix of the first observation 5×5.

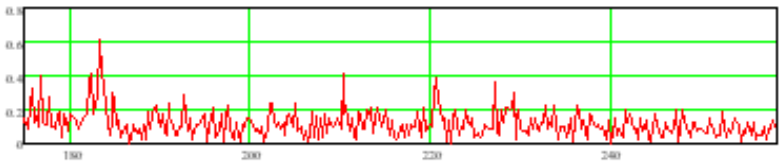

Fig. 10. The amplitude of the module of the Fourier spectrum of the filtered data of the second range of first observation in relative units, in the frequency range. from 170 to 250 Hz. The frequency in Hertz is given on the abscissa. The y-axis shows the range amplitude in relative units

The Figure 11 shows the Fourier amplitude of the filtered data of the first range of the first observation. The energy of each of the twenty subbands was presented in a matrix of the first observation 5×5.

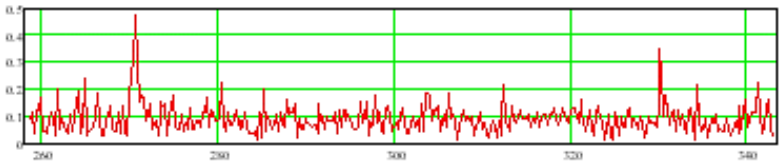

Fig. 11. The amplitude of the module of the Fourier spectrum of the filtered data of the second range of first observation in relative units, in the frequency range from 250 to 330 0 Hz. The frequency in Hertz is given on the abscissa. The y-axis shows the range amplitude in relative units

ISSN 2707-1758

The Figure 12 shows the Fourier amplitude of the filtered data of the first range of the first observation. The energy of each of the twenty subbands was presented in a matrix of the first observation 5×5.

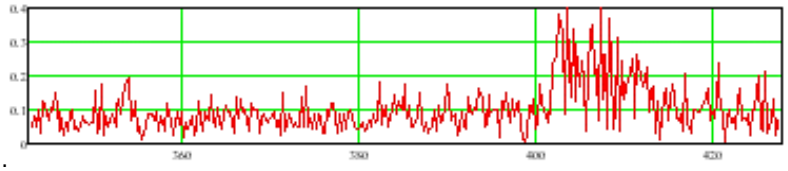

Fig. 12. The amplitude of the module of the Fourier spectrum of the filtered data of the second range of first observation in relative units, in the frequency range from 340 to 420 Hz. The frequency in Hertz is given on the abscissa. The y-axis shows the range amplitude in relative units

The Figure 13 shows the amplitude of the module of the Fourier spectrum of the filtered data of the second range of first observation in relative units, in the frequency range from 420 to 500 Hz. The frequency in Hertz is given on the abscissa. The y-axis shows the range amplitude in relative units.

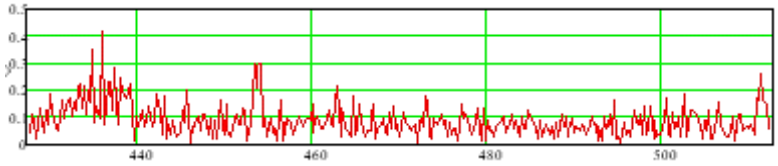

Fig. 13. shows the Fourier amplitude of the filtered data of the first range of the first observation. The energy of each of the twenty subbands was presented in a matrix of the first observation 5×5

The Figure 14 shows the Fourier amplitude of the filtered data of the first range of the first observation. The energy of each of the twenty subbands was presented in a matrix of the first observation 5×5.

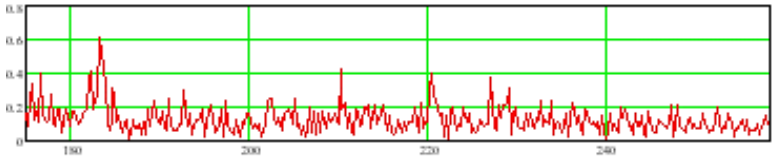

Fig. 14. The amplitude of the module of the Fourier spectrum of the filtered data of the second range of first observation in relative units, in the frequency range from 170 to 250 Hz. The frequency in Hertz is given on the abscissa. The y-axis shows the range amplitude in relative units

The Figure 15 shows the Fourier amplitude of the filtered data of the first range of the first observation. The energy of each of the twenty subbands was presented in a matrix of the first observation 5×5.

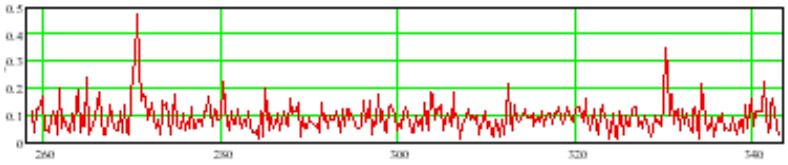

Fig. 15. The amplitude of the module of the Fourier spectrum of the filtered data of the second range of first observation in relative units, in the frequency range from 250 to 330 0 Hz. The frequency in Hertz is given on the abscissa. The y-axis shows the range amplitude in relative units

The Figure 16 shows the Fourier amplitude of the filtered data of the first range of the first observation. The energy of each of the twenty subbands was presented in a matrix of the first observation 5×5.

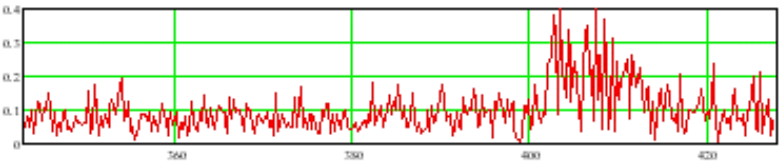

Fig. 16. The amplitude of the module of the Fourier spectrum of the filtered data of the second range of first observation in relative units, in the frequency range from 340 to 420 Hz. The frequency in Hertz is given on the abscissa. The y-axis shows the range amplitude in relative units

The Figure 17 shows the Fourier amplitude of the filtered data of the first range of the first observation. The energy of each of the twenty subbands was presented in a matrix of the first observation 5×5. The energy of each of the twenty sub bands was presented in a matrix 5×5, table 1.

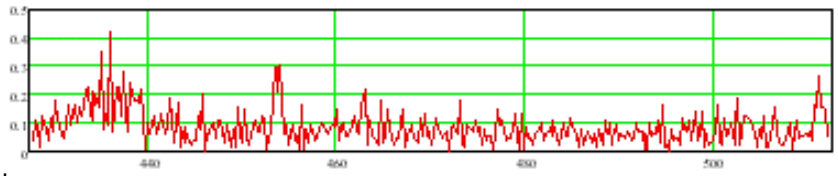

Fig. 17. The amplitude of the module of the Fourier spectrum of the filtered data of the second range of first observation in relative units, in the frequency range from 420 to 500 Hz. The frequency in Hertz is given on the abscissa. The y-axis shows the range amplitude in relative units

Table 1

Matrix of energy size 5×5 of quintiles of all 25 subbands of the first observation of the first observation

2.3054	2.7727	1.8019	1.2790	2.1570
2.1405	1.8973	1.4254	1.2361	1.5053
2.5438	2.2818	1.5132	1.3459	1.3412
2.1597	2.0464	1.4520	2.7071	1.0495
2.2884	1.5792	1.5325	1.6143	1.2925

The second observation. To assess the dynamics of the emission intensity generated by cracking in the observation area, we will carry out the second observations using the parametric model (1–4) to study building № 3 (cell) of the Kyiv Pechersk Lavra.

The second observation of the building № 3 (cell) of the Kyiv Pechersk Lavra is given below.

Data registration during seismic-acoustic monitoring is accompanied by simultaneous additive interference caused by external factors. This study used frequency filtering for data preprocessing (Mostovoy, S., & Mostovoy, V., 2011).

Figures 18 and 19 show fragments of the recording of the second observation lasting 4 seconds, the response of the building to the natural background, unfiltered (Fig.18) and filtered (Fig. 19).

On the Figure 20 the Amplitude of the module of the Fourier spectrum of the low-pass filtered data is shown.

The frequency range was from 90 Hz to 500 Hz. It was divided into five equal quantiles (4), each into five equal subranges.

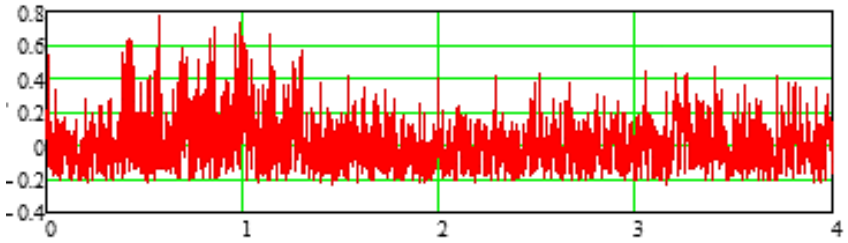

Fig. 18. A fragment of the recording of the second observation (duration 4 seconds) of the building's reaction to the natural background. The abscissa shows time in seconds. Along the ordinate axis, the function of the acceleration of the structure's oscillations in m/sec^2 is plotted with precision to the multiplier

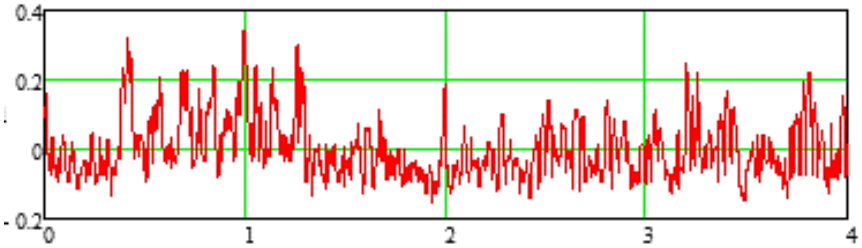

Fig. 19. A fragment of a filtered recording of the second observation (duration 4 seconds) of the building's reaction to the natural background. On the abscissa axis, the time is present in seconds. Along the ordinate axis, the function of the acceleration of oscillation of the structure m/sec^2 is plotted with precision to the multiplier

ISSN 2707-1758

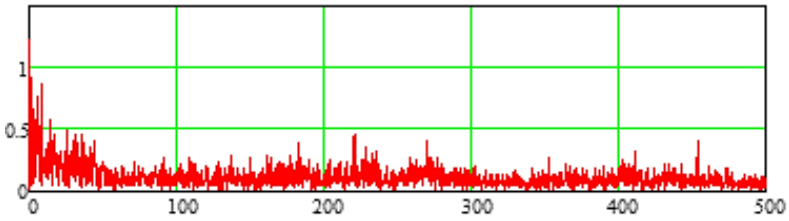

Fig. 20. The amplitude of the module of the Fourier spectrum of the filtered data of the second observation in relative units, in the frequency range from 0 to 600 Hz. The frequency in Hertz is given on the abscissa. The y-axis shows the range amplitude in relative units

The Figure 21 shows the Fourier amplitude of the filtered data of the first range of the first observation. The energy of each of the twenty sub bands was presented in a matrix of the first observation 5×5.

Fig. 21. The amplitude of the module of the Fourier spectrum of the filtered data of the first range of the second observation in relative units, in the frequency range from 90 to 170 Hz. The frequency in Hertz is given on the abscissa. The y-axis shows the range amplitude in relative units

The Figure 22 shows the amplitude of the module of the Fourier spectrum of the filtered data of the first subband of the first band presented in relative units, in the frequency range from 90 to 105 Hz.

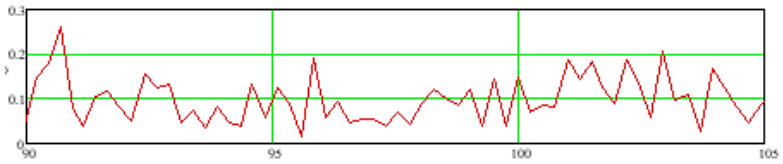

Fig. 22. The amplitude of the module of the Fourier spectrum of the filtered data of the first subband of the first band in relative units, in the frequency range from 90 to 105 Hz. The frequency in Hertz is given on the abscissa. The y-axis shows the range amplitude in relative units

The Figure 23 shows the amplitude of the module of the Fourier spectrum of the filtered data of the second subband of the first band presented in relative units, in the frequency range from 105 to 125 Hz.

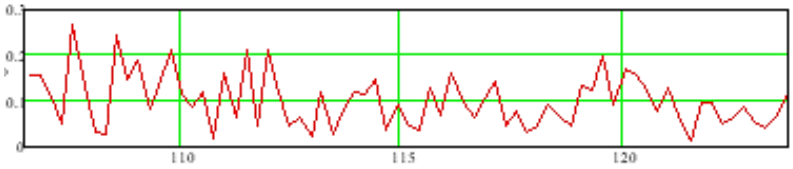

Fig. 23. The amplitude of the module of the Fourier spectrum of the filtered data of the second subband of the first band in relative units, in the frequency range from 105 to 125 Hz. The frequency in Hertz is given on the abscissa. The y-axis shows the range amplitude in relative units

The Figure 24 shows the amplitude of the module of the Fourier spectrum of the filtered data of the third subband of the first band presented in relative units, in the frequency range from 125 to 140 Hz.

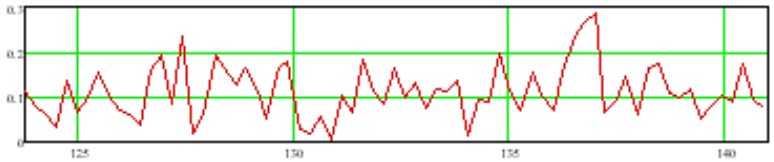

Fig. 24. The amplitude of the module of the Fourier spectrum of the filtered data of the third subband of the first band in relative units, in the frequency range from 125 to 140 Hz. The frequency in Hertz is given on the abscissa. The y-axis shows the range amplitude in relative units

The Figure 25 shows the amplitude of the module of the Fourier spectrum of the filtered data of the fourth subband of the first band presented in relative units, in the frequency range from 140 to 155 Hz.

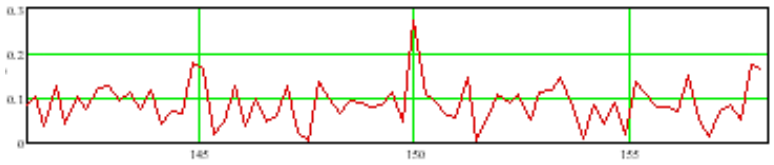

Fig. 25. The amplitude of the module of the Fourier spectrum of the filtered data of the fourth subband of the first band in relative units, in the frequency range from 140 to 155 Hz. The frequency in Hertz is given on the abscissa. The y-axis shows the range amplitude in relative units

The Figure 26 shows the amplitude of the module of the Fourier spectrum of the filtered data of the fourth subband of the first band presented in relative units, in the frequency range of 155 to 170 Hz.

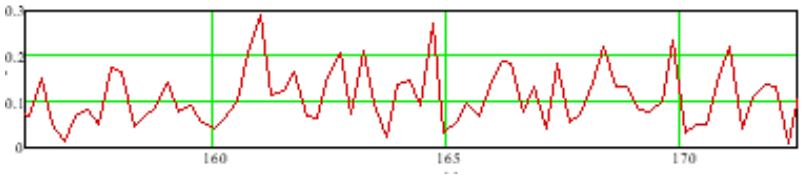

Fig. 26. The amplitude of the module of the Fourier spectrum of the filtered data of the fourth subband of the first band in relative units, in the frequency range from 155 to 170 Hz. The frequency in Hertz is given on the abscissa. The y-axis shows the range amplitude in relative units

The Figure 27 shows the Fourier amplitude of the filtered data of the first range of the second observation. The energy of each of the twenty subbands was presented in a matrix of the first observation 5×5.

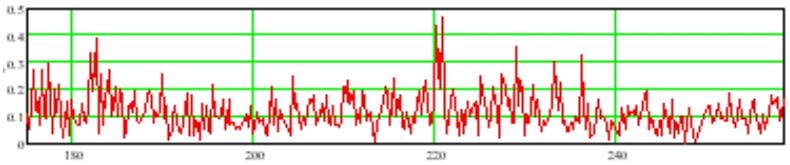

Fig. 27. The amplitude of the module of the Fourier spectrum of the filtered data of the second range of first observation in relative units, in the frequency range from 170 to 250 Hz. The frequency in Hertz is given on the abscissa. The y-axis shows the range amplitude in relative units

The Figure 28 shows the Fourier amplitude of the filtered data of the first range of the second observation. The energy of each of the twenty subbands was presented in a matrix of the first observation 5×5.

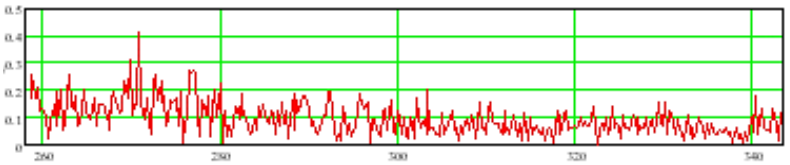

Fig. 28. The amplitude of the module of the Fourier spectrum of the filtered data of the second range of first observation in relative units, in the frequency range from 250 to 330 0 Hz. The frequency in Hertz is given on the abscissa. The y-axis shows the range amplitude in relative units

The Figure 29 shows the Fourier amplitude of the filtered data of the first range of the second observation. The energy of each of the twenty subbands was presented in a matrix of the first observation 5×5.

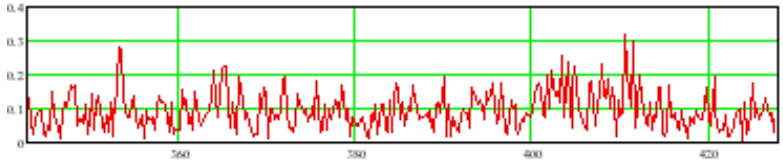

Fig. 29. The amplitude of the module of the Fourier spectrum of the filtered data of the second range of first observation in relative units, in the frequency range from 340 to 420 Hz. The frequency in Hertz is given on the abscissa. The y-axis shows the range amplitude in relative units

ISSN 2707-1758

The Figure 30 shows the Fourier amplitude of the filtered data of the first range of the second observation. The energy of each of the twenty subbands was presented in a matrix of the first observation 5×5, table 2.

Similarly, the energy matrix of 25 subbands was obtained for the second recording fragment.

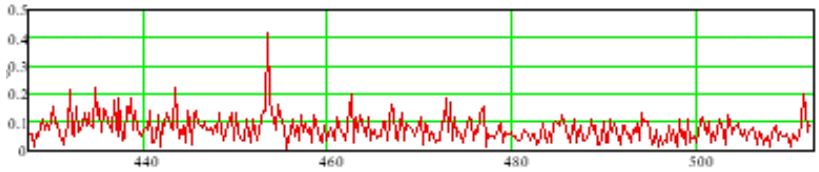

Fig. 30. The amplitude of the module of the Fourier spectrum of the filtered data of the second range of first observation in relative units, in the frequency range from 420 to 500 Hz. The frequency in Hertz is given on the abscissa. The y-axis shows the range amplitude in relative units

Table 2

Matrix of the energy size 5×5 of the quantiles of all 25 subbands of the second fragment of the recording Fig. 14

2.2574	2.7012	1.7931	1.3520	2.2752
2.0735	1.9259	1.4074	1.2935	1.4875
2.4780	2.2015	1.4257	1.3129	1.4590
2.2745	2.6549	1.9350	2.0250	1.1487
2.3582	1.6940	1.7253	1.1542	1.9537

Discussion and conclusions

The strength characteristics of any object depend on its spectral characteristics, that is, the possibility of propagation of elastic waves with different parameters. The structural failure of the material consists in the loss of the load-bearing capacity of the element or directly of the entire structure. It begins when the stresses in the material approach the limit, causing excessive deformations, when the material does not return to its initial state during the entire cycle. Cyclic stresses should lead to material fatigue. Fatigue leads to irreversible deformations. The aging process in the proposed model is a change in material parameters reflected in the feature space.

It is advisable to use emission dynamics to assess the dynamics of high-frequency signals generated by cracks that arise during the structure's operation. For an adequate assessment of the emission dynamics generated by microcracks, it is natural to use an algorithm based on the theorem for processes that are stationary in the sense of (1)–(3). Two stages of the study of the dynamics of the emission of the building are generated by the occurrence of microcracks using the algorithm based on the theorem for processes that are stationary in the sense of (1)–(3). Showed that for a given time interval, the change in emission characteristics was reflected in the energy size matrix of the quantiles of all 25 subbands of each of the two research fragments, Fig. 1, 2.

For an adequate assessment of the emission dynamics generated by cracks that occur during the operation of the structure, it is necessary to collect statistics on a time interval of decades. To solve this problem, it is necessary to carry out permanent seismшс-acoustic monitoring of the building structure.

The authors acknowledge the funding received by the National Research Foundation of Ukraine from the state budget 2022.01/0209 "Complex research of the geoecological state of preservation of the historical and cultural heritage objects of the National Reserve "Kyiv-Pechersk Lavra" in the conditions of military operations" (NRFU Competition "Science for the Recovery of Ukraine in the War and Post-War Periods").

References

Mostovoy, S., & Mostovoy, V. (2011). Problems of filtration at geophysical information processing. *Geoinfomatika*, 2, 48–52 [in Ukranian]. [Мостовой, С., & Мостовой, В. (2011). Проблеми фільтрації при обробці геофізичної інформації. *Геоінфоматика*, 2, 48–52].

Mostovoy, V., & Mostovoy, S. (2023). Models of optimization of dynamic parameters of the object in passive monitoring. *Cybersecurity: Education, Science, Technology,* 28(5), 112–123 [in Ukranian]. [Мостовой, В., & Мостовой, С. (2023). Моделі оптимізації динамічних параметрів об'єкта при пасивному моніторингу. *Кібербезпека: освіта, наука, техніка,* 28(5), 112–123].

Mostovyy, V. (2013). *Models of geophysical field monitoring systems* [Dissertation for the degree of Doctor of Physical and Mathematical Sciences] Kyiv National University of Construction and Architecture [in Ukranian]. [Мостовий, В. (2013). Моделі систем геофізичного моніторингу поля [Дис. д-ра фіз.-мат. наук] Київський національний університет будівництва і архітектури.

Schijve, J. (2003). Fatigue of structures and materials in the 20th century and the state of the art. *International Journal of Fatigue*, 25(8), 679–702.

Suresh, S. (2004). *Fatigue of Materials*. Cambridge University Press.

Tassios T. (2010). Seismic engineering of monuments. *Bulletin of earthquake engineering*, 8(6), 1231–1265.

Timoshenko, S., & Gere, J. (1961). *Theory of elastic stability* (2nd ed). McGraw-Hill.

Отримано редакцією журналу / Received: 01.12.24
Прорецензовано / Revised: 05.12.24
Схвалено до друку / Accepted: 08.12.24

Василь МОСТОВИЙ, д-р фіз-мат. наук, провід. наук. співроб.
ORSID ID: 0000-0002-1759-1893
e-mail: vasyl.mostovyy@gmail.com
Київський національний університет імені Тараса Шевченка, Київ, Україна

МАТЕМАТИЧНА МОДЕЛЬ ДИНАМІКИ ВИПУСКАННЯ СИГНАЛУ В СИСТЕМАХ СЕЙСМОАКУСТИЧНОГО МОНІТОРИНГУ БУДІВЕЛЬНИХ КОНСТРУКЦІЙ

В с т у п . ***Представлено математичну модель автоматизованих систем сейсмоакустичного моніторингу будівельних конструкцій, яка дозволить оцінити динаміку утворення тріщин у будівельних конструкціях із метою попередження руйнування досліджуваних об'єктів. Сейсмоакустичне поле, яке генерують об'єкти дослідження, відображається в матрицю інформативних параметрів, динаміка якої характеризує динаміку стану об'єкта. Для оцінювання динаміки високочастотних сигналів, які генеруються тріщинами, що виникають у процесі експлуатації споруди, доцільно використовувати динаміку емісії, яку породжують ці сигнали. Для цього, з погляду фізичної доцільності, має сенс вибору моделі, яка характеризує динаміку високочастотного діапазону спектра. А саме, в роботі представлено алгоритм, заснований на теоремі для стаціонарних у широкому сенсі процесів.***

М е т о д и . ***Процес старіння може бути відображений у простір ознак, який може бути зведений до множини параметрів, що характеризують пружні властивості матеріалів, які формують досліджувані об'єкти. Оскільки швидкості розповсюдження та форма поздовжніх і поперечних хвиль у матеріалі залежать від пружних параметрів цих матеріалів (коефіцієнта Пуассона та модуля Юнга), то зміна вказаних параметрів призводить до змін спектральних характеристик емісійних сигналів, які виникають у старіючому матеріалі. Будь-який перерозподіл енергії у матеріалі супроводжується виникненням сигналів, що генерують емісію. Динаміка параметрів сигналу емісії відображає зміну пружних властивостей досліджуваного об'єкта. Можливі причини змін внутрішньої структури – це виникнення та збільшення тріщин, фазові переходи в монолітних матеріалах і розпушення складових. Це означає, що зміни динамічних параметрів сигналів емісії пов'язані з динамічними характеристиками вказаного об'єкта.***

Р е з у л ь т а т и . ***Запропоновано математичну модель старіння будівельної конструкції. Ця модель старіння об'єкта має враховувати природу зовнішніх впливів на об'єкт і природу його реакції на зовнішні збурення. З урахуванням наявності стохастичного фонового шуму під час моніторингу, у моделі слід прийняти лише статистичний характер цієї залежності. Вказану модель реалізовано на корпусі № 3 (келії) Києво-Печерської лаври.***

В и с н о в к и . ***Два етапи дослідження динаміки емісії корпусу № 3 Києво-Печерської лаври показали, що за даний інтервал часу зміна характеристик емісії цього об'єкта перебуває в межах похибки вимірювання. Отже, для адекватного оцінювання динаміки емісії, що генерується тріщинами, які виникають у процесі експлуатації корпусу № 3 Києво-Печерської лаври, необхідно використовувати статистику на інтервалі часу в кілька десятиліть. Для розв'язання цієї задачі необхідно проводити постійний сейсмоакустичний моніторинг будівельної конструкції.***

К л ю ч о в і с л о в а : ***сейсмоакустичний моніторинг, сейсмоакустична емісія, математична модель, сейсмоакустичний сигнал, матриця інформативних параметрів моделі, старіння конструкцій.***

Автор заявляє про відсутність конфлікту інтересів. Спонсори не брали участі в розробленні дослідження; у зборі, аналізі чи інтерпретації даних; у написанні рукопису; в рішенні про публікацію результатів.

The author declares no conflicts of interest. The funders had no role in the design of the study; in the collection, analyses or interpretation of data; in the writing of the manuscript; in the decision to publish the results.